# Correction

**EARTH, ATMOSPHERIC, AND PLANETARY SCIENCES**

Correction for "Anthropogenic and biogenic $CO_2$ fluxes in the Boston urban region," by Maryann Sargent, Yanina Barrera, Thomas Nehrkorn, Lucy R. Hutyra, Conor K. Gately, Taylor Jones, Kathryn McKain, Colm Sweeney, Jennifer Hegarty, Brady Hardiman, and Steven C. Wofsy, which was first published July 2, 2018; 10.1073/pnas.1803715115 (*Proc Natl Acad Sci USA* 115:7491–7496).

The authors note that Jonathan A. Wang should be added to the author list between Brady Hardiman and Steven C. Wofsy. Jonathan A. Wang should be credited with contributing new reagents/analytic tools. The corrected author line, affiliation line, and author contributions appear below. The online version has been corrected.

**Maryann Sargent[a,1], Yanina Barrera[a], Thomas Nehrkorn[b], Lucy R. Hutyra[c], Conor K. Gately[a,c], Taylor Jones[a], Kathryn McKain[d], Colm Sweeney[d], Jennifer Hegarty[b], Brady Hardiman[c,e], Jonathan A. Wang[c], and Steven C. Wofsy[a]**

[a]School of Engineering and Applied Sciences, Harvard University, Cambridge, MA 02138; [b]Atmospheric and Environmental Research, Inc., Lexington, MA 02421; [c]Department of Earth and Environment, Boston University, Boston, MA 02215; [d]Global Monitoring Division, Earth System Research Laboratory, National Oceanic and Atmospheric Administration, Boulder, CO 80305; and [e]Department of Environmental and Ecological Engineering, Purdue University, West Lafayette, IN 47907

Author contributions: T.N., L.R.H., and S.C.W. designed research; M.S., Y.B., T.N., C.K.G., K.M., C.S., J.H., B.H., and S.C.W. performed research; T.J., K.M., and J.A.W. contributed new reagents/ analytic tools; M.S., Y.B., C.K.G., B.H., and S.C.W. analyzed data; and M.S. wrote the paper.



Published online September 24, 2018.

www.pnas.org/cgi/doi/10.1073/pnas.1815348115

CORRECTION

# Anthropogenic and biogenic $CO_2$ fluxes in the Boston urban region

Maryann Sargent[a,1], Yanina Barrera[a], Thomas Nehrkorn[b], Lucy R. Hutyra[c], Conor K. Gately[a,c], Taylor Jones[a], Kathryn McKain[d], Colm Sweeney[d], Jennifer Hegarty[b], Brady Hardiman[c,e], Jonathan A. Wang[c], and Steven C. Wofsy[a]

[a]School of Engineering and Applied Sciences, Harvard University, Cambridge, MA 02138; [b]Atmospheric and Environmental Research, Inc., Lexington, MA 02421; [c]Department of Earth and Environment, Boston University, Boston, MA 02215; [d]Global Monitoring Division, Earth System Research Laboratory, National Oceanic and Atmospheric Administration, Boulder, CO 80305; and [e]Department of Environmental and Ecological Engineering, Purdue University, West Lafayette, IN 47907

Edited by Ronald C. Cohen, University of California, Berkeley, CA, and accepted by Editorial Board Member A. R. Ravishankara May 25, 2018 (received for review March 5, 2018)

**With the pending withdrawal of the United States from the Paris Climate Accord, cities are now leading US actions toward reducing greenhouse gas emissions. Implementing effective mitigation strategies requires the ability to measure and track emissions over time and at various scales. We report $CO_2$ emissions in the Boston, MA, urban region from September 2013 to December 2014 based on atmospheric observations in an inverse model framework. Continuous atmospheric measurements of $CO_2$ from five sites in and around Boston were combined with a high-resolution bottom-up $CO_2$ emission inventory and a Lagrangian particle dispersion model to determine regional emissions. Our model–measurement framework incorporates emissions estimates from submodels for both anthropogenic and biological $CO_2$ fluxes, and development of a $CO_2$ concentration curtain at the boundary of the study region based on a combination of tower measurements and modeled vertical concentration gradients. We demonstrate that an emission inventory with high spatial and temporal resolution and the inclusion of urban biological fluxes are both essential to accurately modeling annual $CO_2$ fluxes using surface measurement networks. We calculated annual average emissions in the Boston region of 0.92 kg $C{\cdot}m^{-2}{\cdot}y^{-1}$ (95% confidence interval: 0.79 to 1.06), which is 14% higher than the Anthropogenic Carbon Emissions System inventory. Based on the capability of the model–measurement approach demonstrated here, our framework should be able to detect changes in $CO_2$ emissions of greater than 18%, providing stakeholders with critical information to assess mitigation efforts in Boston and surrounding areas.**

greenhouse gas emissions | inverse modeling | carbon dioxide | biogenic fluxes

Carbon dioxide ($CO_2$) emissions from fossil fuels are the dominant anthropogenic contributor to climate change (1). Urban areas account for the majority of global fossil fuel $CO_2$ emissions (2), and their contribution is expected to rise as the urban population grows from the current 3.6 billion to an expected 6 billion by 2050 (3). Due to the pending withdrawal of the United States from the Paris climate accord, cities and states across the nation are taking the lead in efforts to reduce greenhouse gas (GHG) emissions, with 323 cities, including Boston, committing to emission reduction targets (4). Because urban emissions are spatially concentrated and distinct in both spatial scale and governance, urban areas provide a unique test bed to assess GHG mitigation strategies.

Verification of reported emissions and tracking over time are essential to assessing the efficacy of GHG mitigation efforts. Carbon emissions can be estimated using "bottom-up" and/or "top-down" methods, which are complementary to each other. Bottom-up methods convolve reported fossil fuel usage from various source sectors with the carbon content of the fuel (5, 6), while top-down methods quantify emissions based on GHG concentration gradients measured in the atmosphere. Bottom-up emissions estimates are limited in their ability to detect trends because methodologies and available input data may change between assessments of different years. Uncertainties are also difficult to quantify due to the coarse scale of emissions reporting data and a lack of error estimates in the reporting data, including emissions factors, activities, and spatial distributions (7). Atmospheric GHG concentrations alone are also unreliable for resolving trends in emissions because they are highly dependent on wind patterns and weather, which vary from year to year.

Here, we develop a top-down assessment based on inverse modeling, which provides a straightforward approach to quantifying uncertainties in emissions for the detection of trends due to policy, regulation, or economic changes. The inverse model can also serve to evaluate bottom-up inventories. Urban GHG monitoring projects are underway in many cities, including Los Angeles (8), Indianapolis (9), Salt Lake City (10), Paris (11), Washington, DC (12), and Boston (13). These observational networks provide an opportunity for top-down assessments of GHG emissions using high-precision atmospheric measurements that are highly intercomparable both within the network and between networks, and offer long-term stability. Important work has been done in each of these cities to design optimal sensor placement, characterize $CO_2$ enhancements, and determine the $CO_2$ concentrations at the boundaries of the study region (14, 15). Community-wide efforts are also underway to harmonize city-scale observational networks and inverse modeling across the United States (16) and internationally (17).

## Significance

Cities are taking a leading role in US efforts to reduce greenhouse gas emissions, and require traceable methods to assess the efficacy of their efforts. In this study, we developed an inverse model framework that quantified emissions in the Boston urban region over 16 months and is capable of detecting changes in emissions of greater than 18%. We show that a detailed representation of urban biological fluxes and knowledge of the spatial and temporal distribution of emissions are essential for accurate modeling of annual $CO_2$ emissions. Across the globe, it is possible to quantifiably assess the efficacy of mitigation efforts by developing frameworks similar to the one we present here for Boston.

Author contributions: T.N., L.R.H., and S.C.W. designed research; M.S., Y.B., T.N., C.K.G., K.M., C.S., J.H., B.H., and S.C.W. performed research; T.J., K.M., and J.A.W. contributed new reagents/analytic tools; M.S., Y.B., C.K.G., B.H., and S.C.W. analyzed data; and M.S. wrote the paper.

The authors declare no conflict of interest.

This article is a PNAS Direct Submission. R.C.C. is a guest editor invited by the Editorial Board.



Data deposition: The data reported in this paper have been deposited in the Oak Ridge National Laboratory (https://doi.org/10.3334/ORNLDAAC/1501, https://doi.org/10.3334/ORNLDAAC/1572, https://doi.org/10.3334/ORNLDAAC/1586, and https://doi.org/10.3334/ORNLDAAC/1596).

[1]To whom correspondence should be addressed. Email: mracine@fas.harvard.edu.

This article contains supporting information online at www.pnas.org/lookup/suppl/doi:10.1073/pnas.1803715115/-/DCSupplemental.

Published online July 2, 2018.

To date, few studies have rigorously quantified urban emissions based on long-term atmospheric measurements. Lauvaux et al. (9) reported that total emissions from Indianapolis in the 2012–2013 dormant season were 20% higher than the Hestia inventory; this study included only anthropogenic emissions, and not biogenic fluxes. Staufer et al. (11) included anthropogenic and nonurban biogenic fluxes over a full year in Paris, France, and estimated that emissions were 20% lower than the Airparif inventory. Only periods with wind directions within ±15° of the Paris transect from upwind to downwind sites were included, limiting the available data to 8% of collected hours. We present a top-down study to quantify urban emissions for over a full year. We show that detailed spatial and temporal representations of anthropogenic emissions and both urban and rural biological fluxes must be employed.

## Model and Measurement Framework

We quantified $CO_2$ emissions in the Boston urban region from September 2013 to December 2014 by modeling the changes in $CO_2$ concentrations as air traveled from the boundary, a 90-km radius around Boston, to our two sites in the urban core (Fig. 1). A single multiplicative scaling factor (SF) was calculated for the prior anthropogenic emissions in each season to best match the observed atmospheric gradient. The modeled $CO_2$ enhancement ($\Delta CO_2$) expected from the prior emissions was determined using the Hybrid Single-Particle Lagrangian Integrated Trajectory (HYSPLIT) model (18), which followed an ensemble of 1,000 particles released at the urban measurement sites backward in time based on wind fields and turbulence from the North American Mesoscale Forecast System (NAM) at 12-km resolution. Although meteorological driver fields are at 12-km resolution, Lagrangian particle dispersion models such as HYSPLIT can simulate transport on a finer scale because particle locations are not restricted to a grid and meteorological fields are interpolated to subgrid-scale locations. HYSPLIT produces an influence function known as the "footprint" (units: parts per million $CO_2$ per unit flux) that quantifies the particles' sensitivity to surface emissions, linking upwind surface fluxes to changes in atmospheric concentration at the receptor. For comparison, footprints were also calculated using the Stochastic Time-Inverted Lagrangian Transport (STILT) model driven by wind fields from the Weather Research and Forecasting (WRF) mesoscale meteorological model at 1.33-km resolution in the near field (19, 20). (See *SI Appendix*, sections S4 and S5 for further details and validation of both the WRF–STILT and NAM–HYSPLIT models.) A more explicit calculation of mixing layer height in HYSPLIT and STILT was implemented near the urban measurement sites to more accurately account for particle interaction with the surface before they became fully mixed through the planetary boundary layer (PBL) (*SI Appendix*, section S3, Figs. S7 and S8, and Table S4).

The footprints were convolved with a prior emissions estimate based on the sum of the 1-km, 1-h resolution Anthropogenic Carbon Emissions System (ACES) inventory (21) and the urban-Vegetation Photosynthesis Respiration Model (urbanVPRM) (22). The ACES inventory includes all major carbon-emitting sectors using an extensive database of high-resolution spatial proxies, including archived data of roadway-level vehicle traffic (21, 23) as well as human respiration. UrbanVPRM combines satellite-derived land surface greenness, impervious surface area data, and field measurements of aboveground biomass and productivity in urban plots to produce a detailed representation of urban and nonurban biological fluxes in Massachusetts. This model represents a significant improvement over existing biological flux models that are based on data from the Moderate Resolution Imaging Spectroradiometer (MODIS) satellite, which fails to retrieve images of vegetation in urban areas and therefore assigns no biological flux there (*SI Appendix*, Fig. S1). The convolution of footprints and prior fluxes weights the grid cells in the flux models according to their influence on the measured $CO_2$ enhancement at the urban site.

The observed $\Delta CO_2$ was calculated from the difference between urban measurements at Boston University (BU) or Copley Square (COP) and estimates of $CO_2$ concentrations in air entering the urban domain, based on measurements at Harvard Forest in Petersham, MA (HF), Canaan, NH (CA), or Martha's Vineyard, MA (MVY) (Fig. 1 and *SI Appendix*, section S1 and Table S1). The urban sites at BU and COP are only 1.7 km apart but sample at 29 m and 215 m above ground level, respectively, providing a direct observation of the surface layer vertical gradient. The upstream site assigned to each particle was chosen based on the azimuth at which the particle exited the 90-km radius circle around Boston (*SI Appendix*, section S3) as it traveled backward in time. $CO_2$ concentrations measured at HF and CA typically agree well (*SI Appendix*, Table S2 provides $R^2$ and RMSE for pairs of background sites), indicating that they are representative of the air in the region absent influence of the urban center.

Measurements made during times of easterly flow (exit azimuth 0° to 120°) were discarded due to greater uncertainty in modeling sea breezes and lack of a suitable boundary site. We compared the use of all exit angles between sites, except for east winds, with constraints allowing only particles which exited within a certain angle of each site. We found the best model–measurement agreement using exit angles within ±40° of HF or CA, excluding winds from the direction of the MVY site, which are more difficult to model; this was the condition used in *Results* (comparisons including the MVY site were also very good, and are shown in *SI Appendix*, section S6 and Table S5). A time delay between the upwind and downwind sites was used based on the travel time of each released particle to the edge of the 90-km circle.

There is significant diurnal variability in $CO_2$ concentrations of air entering the urban domain, with two causes: variability of the PBL height and diel variations of upwind fluxes, particularly biogenic fluxes during the growing season (Fig. 2). Additionally, our boundary sites sample at 29 m to 100 m above ground level, but particles released at the urban sites exit the domain at a range of heights, typically from 200 m to 700 m above ground, and there is a significant gradient in atmospheric $CO_2$ concentration across those altitudes. These factors present a unique challenge when estimating boundary $CO_2$ concentrations. To address these issues, we implemented a method for calculating the $CO_2$ concentration of air entering the urban domain by constructing a vertical $CO_2$ profile from the observations at each boundary site. The site at HF samples just above the tree canopy, where uptake of $CO_2$ by the

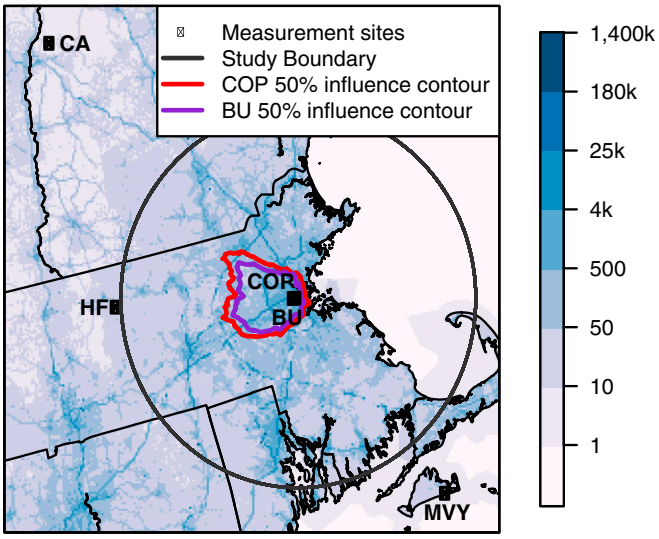


**Fig. 1.** Map of measurement stations in the Boston network including two urban sites: BU, 29-m height, and COP, 215-m height; and three boundary sites: HF, CA, and MVY. Blue shading represents 2014 average afternoon $CO_2$ emissions. The 90-km-radius circle bounds the region in which emissions were optimized. The red (purple) contour encloses 50% of the average 2014 footprint (sensitivity area) initiated at the COP (BU) site and including only wind directions within ±40° of the HF or CA boundary sites.

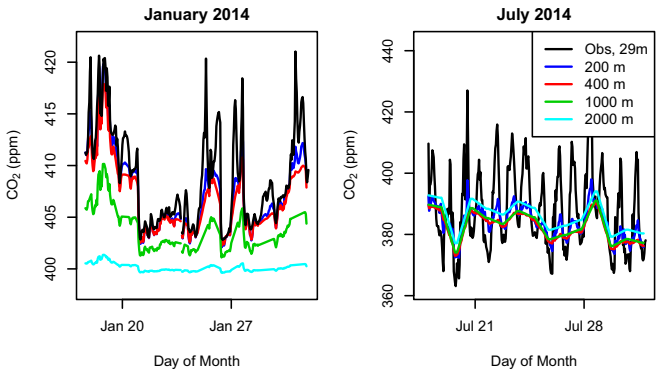


**Fig. 2.** Observed $CO_2$ concentration at HF (black) and calculated boundary concentration as a function of altitude for (*Left*) January 2014 and (*Right*) July 2014.

forest can lead to a significant vertical gradient in the surface layer during summertime. Following Potosnak et al. (24), we used eddy flux measurements made at the same location to adjust measured $CO_2$ concentrations at 29 m to their expected value at 200 m, the top of the stratified surface layer (*SI Appendix*, section S3 and Fig. S2). In our boundary curtain, $CO_2$ concentrations at HF exponentially increased from the observed value at 29 m to the flux-corrected PBL value between 29 and 200 m. At CA and MVY, tower measurements were taken as representative of the ground to 200 m.

Above 200 m at all sites, we constructed $CO_2$ profiles using monthly mean vertical gradients from Carbon Tracker CT2015 (CT) (25) (*SI Appendix*, Fig. S4), adjusted as described below to match our measurement-based estimate at 200 m. We tested this approach by comparing CT profiles to aircraft flask profiles, and found that CT showed good agreement with the observed gradients (*SI Appendix*, Fig. S3). During the growing season, afternoon CT profiles show no change in concentration from the surface to ∼1,000 m; we therefore apply observed $CO_2$ concentrations to all levels up to 1,000 m in the afternoon. Nighttime and morning concentrations at the towers are elevated relative to afternoon observations, but, with increasing altitude, they decrease toward observed afternoon concentrations at a rate determined by CT profiles. In the winter, in addition to this decrease in nighttime concentration toward afternoon values, an additive offset of typically less than 3 ppm was applied with altitude at all hours (*SI Appendix*, section S2). Fig. 2 shows example winter and summer boundary profiles at HF, including both the flux correction and CT-based altitude adjustment. The boundary $CO_2$ concentration for each Lagrangian particle was then determined based on the altitude at which the particle exited the study region, and all particle contributions were averaged.

Modeled $CO_2$ was calculated as the sum of boundary $CO_2$ and modeled $\Delta CO_2$,

$$CO_2[\text{model}] = CO_2[\text{boundary}] + \text{footprint} * \text{prior inventory}$$

Optimized emissions were determined for each season by calculating a multiplicative SF for prior anthropogenic emissions that gives the best fit to observed afternoon $CO_2$ concentrations. SF was determined by dividing the mean observed anthropogenic enhancement for all afternoons in a given season by the mean modeled anthropogenic enhancement:

$$\text{SF} = \text{mean}(CO_2[\text{obs, urban}] - CO_2[\text{boundary}] - \Delta CO_2[bio])/\text{mean}(\Delta CO_2[anthrop])$$

$$\text{optimized emissions} = \text{SF} * \text{prior emissions}$$

Uncertainties in optimized emissions were calculated through a bootstrap analysis that accounted for variations of hourly and daily observed and model enhancements and boundary $CO_2$, as well as uncertainties in prior emissions and atmospheric transport (*SI Appendix*, section S9).

## Results

We quantified average annual anthropogenic emissions in the study region to be 0.92 kg $C{\cdot}m^{-2}{\cdot}y^{-1}$ [0.79 to 1.06, 95% CI] based on the average of results from the BU and COP sites. Prior emissions were scaled by a factor of 1.14 [+0.18,−0.16, 95% CI] for the full study period, and by 1.04 [+0.19,−0.16] in the winter (Fig. 3). The 18% model uncertainty is somewhat higher than the stated 8.6% uncertainty in the prior ACES inventory; however, the inverse model uncertainty is more comprehensive than the bottom-up inventory uncertainty, which reflects uncertainties in the raw data sources, but not the uncertainties in emissions factors or in downscaling methods which are difficult to quantify. We expect our inverse model framework to be capable of detecting changes in emissions on the order of the model uncertainty, 18%.

We optimized emissions separately based on observations from each site, and adjusted emissions with a single mean SF in each season for all hours and grid cells. A benefit of this method is that the very good model−measurement correlation (Fig. 4 and *SI Appendix*, Fig. S14; $R^2 = 0.67$ for daily afternoon averages, $R^2 = 0.81$ for 7-d running average) is independent of the scaling of emissions, and demonstrates the fidelity of the model in reproducing daily and weekly variability. We focused the optimization on measurements in the urban core during afternoon hours [1100 hours to 1600 hours local time (LT)], when the atmosphere is turbulent and relatively well mixed, because the surface influence is less susceptible to uncertainty in the modeled height of the PBL. Particles released from 1100 hours to 1600 hours LT had a mean time to the 90-km boundary of 3.7 h, with 85% of trajectories reaching the boundary within 7 h. Therefore, emissions were optimized from ∼700 hours to 1600 hours LT most days, with the majority of the footprint influence representing ∼9 h to 16 h.

During the summer afternoons, biogenic uptake of $CO_2$ almost completely balanced anthropogenic $CO_2$ emissions. Therefore, we did not attempt to compute SFs for June, July, and August because the model uncertainty is larger than the near-zero average afternoon enhancement (Fig. 5); our data show that these two components of $CO_2$ flux essentially cancel on summer afternoons in Boston.

The results for the SF include only wind directions within ±40° of the HF or CA boundary sites, which account for 48% of the days during the 13-mo optimization period. However, less stringent wind constraints, which excluded only easterly winds and included 70% of days from the study period, produced similar optimized emissions (*SI Appendix*, Table S5). Fig. 1 shows the region

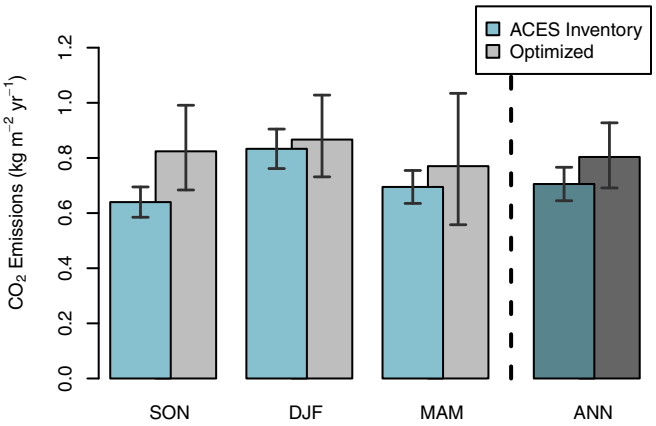


**Fig. 3.** Seasonal prior and optimized anthropogenic $CO_2$ emissions for September 2013 to December 2014 based on the NAM−HYSPLIT model for the average of the BU and COP sites. SON, September to November; DJF, December to February; MAM, March to May; ANN, annual.

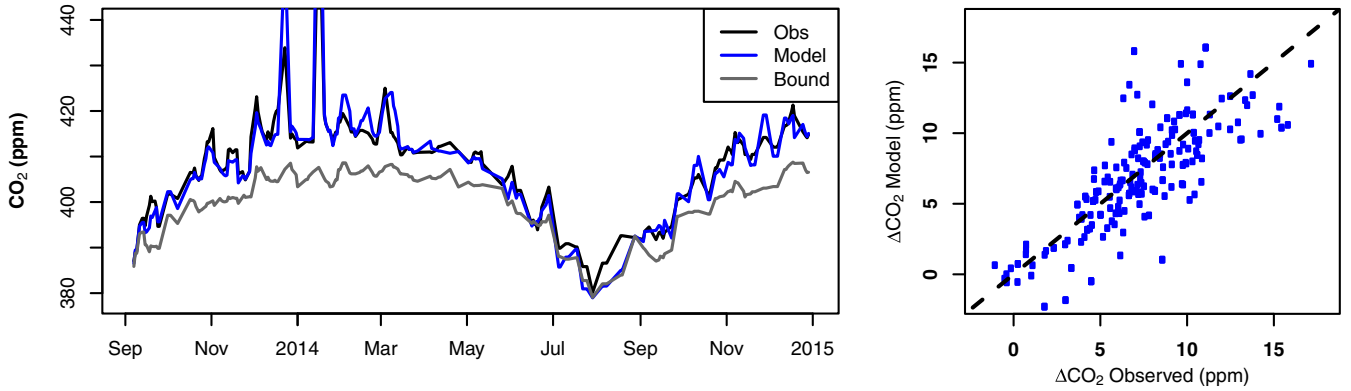


**Fig. 4.** Observed (Obs) , scaled model (Model), and boundary (Bound) $CO_2$ at COP. (*Left*) Seven-day running average afternoon (1100 hours to 1600 hours Eastern Standard Time) concentrations for entire study period, 2013–2014. (*Right*) Modeled vs. observed daily afternoon average $CO_2$ enhancement above boundary concentration for the optimized model, for entire study period, September 2013 to December 2014, excluding June, July, and August. Dashed line is one-to-one.

containing 50% of the footprint, or surface influence, affecting the BU and COP sites, where emissions are best constrained using our model (*SI Appendix*, Fig. S10 compares the footprint influence for different wind selection criteria). The region stretches ∼45 km from Boston, from southwest of the city to northwest of the city.

The model PBL height was the main factor which accounted for differences in calculated footprints for NAM–HYSPLIT and WRF–STILT simulations. To assess the model simulations, we used observations from a Sigma Space Mini Micropulse Lidar (hereafter, "Lidar") located at the BU site, combined with an image processing algorithm, to retrieve daytime PBL heights for the entire study period. While summary verification measures (such as bias, rms error, and correlation coefficients) were comparable for the two models, and similar in magnitude to those found by Lauvaux et al. (9), there were key differences in their error characteristics. In the afternoon, WRF–STILT more often underestimated the PBL height compared with Lidar measurements, leading it to underestimate the afternoon $CO_2$ enhancement at the 215-m COP site (SF > 1) and overestimate the enhancement at the 29-m BU site (SF < 1) (Table 1 and *SI Appendix*, Figs. S11–S13). The WRF–STILT model thus simulates a larger vertical gradient in $CO_2$ concentrations, on average, than exists in the atmosphere in the afternoon. (For further discussion, see *SI Appendix*, section S7.)

We used the SFs from the NAM–HYSPLIT model because it showed better agreement with afternoon Lidar PBL height, leading to better day-to-day correlation with observed $CO_2$ enhancements (*SI Appendix*, Table S6). NAM–HYSPLIT also more accurately captured the atmospheric vertical $CO_2$ gradient between the BU and COP sites, showing no systematic bias with altitude (Table 1 shows no significant difference in SF between the BU and COP sites; see *SI Appendix*, Fig. S16). The NAM–HYSPLIT and WRF–STILT models produced similar optimized emissions in the afternoon after averaging SFs from BU and PRU (Table 1). The sensitivity of these models to PBL height demonstrates that modeled vertical mixing is a source of systematic bias in the calculation of top-down emissions, drawing attention to the need for more accurate vertical mixing and PBL height simulations in models.

This study quantifies emissions using a detailed representation of urban biological fluxes in a top-down framework. In Boston, ACES prior anthropogenic emissions would reproduce observed afternoon $CO_2$ enhancements very well from October to April, but, when plant photosynthetic uptake is active (May to September), anthropogenic enhancements alone are significantly greater than observed enhancements (Fig. 5). Including biological fluxes provided consistent agreement between observations and model across all seasons.

We separated out the impact of the urban biosphere, defined as grid cells where the MODIS net primary productivity (NPP) product did not estimate any biological flux but the urbanVPRM product produces a flux estimate. The urban biosphere alone took up an average 69% of the afternoon anthropogenic enhancement during July in the 90 km around Boston, as measured at COP, and 36% during September. Accounting for urban and nonurban biological activity, the model found that 100% of the afternoon anthropogenic enhancements measured at COP were offset in July, 58% of the enhancement was offset in September, and 20% of the enhancement was offset as late as October. Note that the impact of $CO_2$ uptake by the urban biosphere is amplified at our sites (60 to 70% of the total biological uptake, compared with 11%, on average, in Massachusetts) because they are more strongly influenced by the nearby urban areas than the farther afield suburban and rural areas. As we were not able to calculate an SF in the summer, these results are based on the unscaled model and its overall good agreement with observations (Fig. 5 and *SI Appendix*, Table S6). In the winter, ecosystem respiration produced 17 to 20% of the total $CO_2$ flux in the domain but only 5% of the footprint-scaled enhancement at COP (this does not include human respiration, which we considered anthropogenic emissions). Sensitivities analyses for

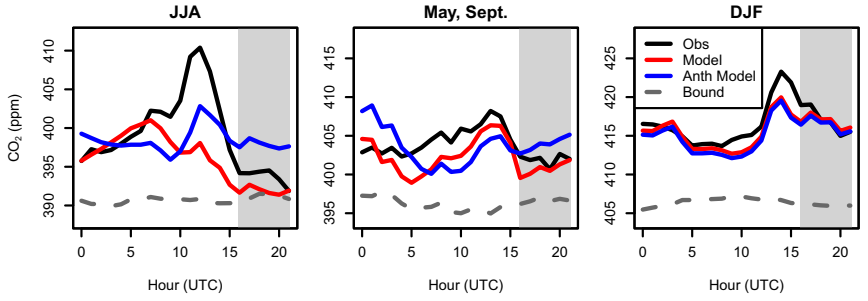


**Fig. 5.** $CO_2$ averaged by hour of the day at COP for (*Left*) June, July, and August; (*Center*) September and May; and (*Right*) December, January, and February. Shown are observations (black), unscaled model including anthropogenic and biogenic fluxes (red), anthropogenic fluxes only model (blue), and boundary (dashed black).

Table 1. SFs for afternoon emissions at BU and COP sites using NAM-HYSPLIT or WRF-STILT models for annual average (excluding summer) and each season

| Season | BU HY | COP HY | All HY | BU WRF | COP WRF | All WRF |
|---|---|---|---|---|---|---|
| ANN | 1.10 | 1.18 | 1.14 [+0.18,−0.16] | 0.78 | 1.49 | 1.15 [+0.41,−0.30] |
| SON | 1.27 | 1.30 | 1.29 [+0.26,−0.22] | 0.75 | 1.34 | 1.05 [+0.47,−0.39] |
| DJF | 1.03 | 1.04 | 1.04 [+0.19,−0.16] | 0.62 | 1.43 | 1.01 [+0.60,−0.47] |
| MAM | 1.01 | 1.19 | 1.11 [+0.38,−0.31] | 1.01 | 1.74 | 1.36 [+0.81,−0.57] |

"All" includes both BU and COP sites, and uncertainty is calculated using the bootstrap method; bracketed values represent 95% confidence intervals.

Indianapolis suggest ecosystem respiration could be as large as 15% of winter flux (26) in that city.

Although summer results were not used to calculate annual SFs, model–observation correlation and mean agreement (Fig. 5 and *SI Appendix*, Table S6) provide confidence in the lack of model bias during the included transitional seasons, when biological fluxes were still important. The inclusion of $CO_2$ uptake from the urban biosphere was therefore essential to accurately calculating emissions in the urban region during the 5 mo of the growing season. Differing from our results, Staufer et al. (11) found that the biogenic signal had only a small impact on inversion results in Paris, but one reason may be that their ecosystem model did not include urban biological fluxes. The seasonal amplitude of their optimized emissions was larger than that of the prior, a result that could, in part, be due to missing biological uptake in the summer.

With a measurement network limited to a small number of urban sites, we cannot strongly constrain the spatial distribution of emissions in the region, and thus we rely on the spatial distribution in the ACES prior inventory. The results are sensitive to the high-resolution spatial information in ACES; using grid sizes greater than 5 km, or insufficiently precise localization of emissions, produced significantly different optimized emissions for Boston. Model results using 1-, 2-, 5-, and 10-km gridded prior inventories showed that SFs increased with grid size (Table 2). If the coarser scale (5 km to 10 km) emissions priors had been used, the modeled $CO_2$ enhancement would have been underestimated by 15 to 30% compared with the higher-resolution model. A flat prior, which averaged emissions over land in rings bounded at 20, 40, and 90 km around Boston, underestimated the $CO_2$ enhancement even more, by ∼50%. (See *SI Appendix*, section S8 and Table S7, for comparison of ACES with other inventories.)

These results show that, for an inverse analysis, the necessary scale of the inventory is dictated by the scale of the footprint near the receptor. With increasing grid size, strong local sources are spread out over a larger area and, if the footprint near the receptor does not cover the larger grid box, the model underestimates the enhancement of $CO_2$ at the receptor. We found little difference between SFs obtained from 1- and 2-km grids, indicating that a 2-km grid is likely small enough to capture the variability in emissions. However, future work such as comparison with higher spatial resolution priors in the near field will be necessary to verify that a 1-km grid sufficiently captures source variability. Small grid sizes are necessary for measurement sites with strong, spatially nonuniform emissions nearby, although not for sites downwind of cities and away from strong emitters. However, measurements at downwind sites are very sensitive to dispersion of the urban plume and to model wind directions, and such sites are not always available. Boston requires the placement of sensors within the city to capture the urban enhancement, as emissions are lofted above the surface layer over the ocean as they exit the city. During times of westerly winds, $CO_2$ concentrations measured at Thompson Island in Boston Harbor typically show enhancements relative to HF of less than half of those observed at PRU.

Some other cities have constructed GHG measurement networks with sensors in the midst of strong urban emissions (8–11). Our results are in agreement with those of Feng et al. (8), who found that a 1.3-km resolution prior inventory better reproduced $CO_2$ variability across Los Angeles than a 10-km prior. We conclude that a spatially explicit prior inventory, with realistic spatial and temporal distributions, and the inclusion of biological fluxes, are necessary features for an accurate assessment of top-down emissions. The inverse modeling approach can then give strong constraints on total emissions in the urban domain.

Our results also demonstrate the importance of an accurate assessment of the $CO_2$ concentrations at the boundary of the study area. We developed a boundary $CO_2$ curtain tied to surface measurements and varying with altitude that produced significantly better agreement with observations than using either a simple difference between surface observations or a curtain from the CT model. Over the entire 16-mo study period, using a simple difference method (accounting for transit time to the receptor but not the vertical gradient in atmospheric $CO_2$) produced an average model $CO_2$ enhancement 57% greater than observations, compared with 18% lower than observations with our upwind boundary curtain. Our boundary curtain and a CT boundary produce similar agreement with observations when averaged over the full year, but the CT boundary data have seasonal biases, leading to model enhancements 25% greater than observations in the winter, 30% greater in March and April, and 50% greater in May and September, compared with 4%, 7%, and 32% lower than observations, respectively, with our upwind boundary curtain (*SI Appendix*, Fig. S15). The efficacy of our boundary curtain was similar for simulations using the WRF–STILT model (*SI Appendix*, section S3). The comparison with CT confirms the importance of using observations to account for CT biases, as also shown for Indianapolis (9) and Paris (15).

We also note that it was very important to include a correction for the surface layer gradients associated with uptake or emission by the forest at the HF site (24), which samples near the forest canopy top. In the growing season, this correction increased afternoon boundary $CO_2$ by 2.6 ppm on average, significantly improving the model fit to observations (*SI Appendix*, Fig. S15). We infer that treatment of surface layer fluxes and gradients is needed when using data from towers in the inversion framework, especially for upwind boundary sites in forests or agricultural areas.

## Conclusions

With the pending withdrawal of the United States from the Paris climate accord, many cities and states have proposed strategies to reduce GHG emissions at the local level. For example, Boston has set a target of reducing GHG emissions to 25% less than 2005 levels by 2020, and becoming carbon neutral by 2050 (27). It will be essential to put in place rigorous measurements of actual emissions to assess the efficacy of these efforts. Bottom-up emissions inventories may change methodologies between assessments with improvement in data availability, and have poorly constrained uncertainties, making them difficult to use for trend

Table 2. SF at COP as function of grid size of prior inventory

| Season | 1 km | 2 km | 5 km | 10 km |
|---|---|---|---|---|
| ANN | 1.18 | 1.16 | 1.41 | 1.39 |
| SON | 1.30 | 1.16 | 1.36 | 1.37 |
| DJF | 1.05 | 1.13 | 1.40 | 1.32 |
| MAM | 1.19 | 1.21 | 1.48 | 1.48 |

detection. However, top-down assessments provide quantifiable uncertainties and may be made consistent over long timescales. As the accuracy of atmospheric transport models improves, our framework allows for transparent retrospective refinements in emissions estimates. This study used 16 mo of $CO_2$ measurements at two sites in Boston and three boundary sites outside the city with a high-resolution modeling framework to quantify average anthropogenic emissions in the region to be 0.92 kg $C{\cdot}m^{-2}{\cdot}y^{-1}$ (95% CI: 0.79 to 1.06), which is 14% higher than that calculated by the ACES inventory. The modeled $CO_2$ enhancement also showed very good correlation with observations on daily and weekly timescales. Using continuous, long-term measurements, we have demonstrated the capability of our model–measurement framework in Boston to detect changes in emissions on the order of 18%, the model uncertainty (95% CI). This network and overall modeling strategy is therefore ready to be applied in Boston to evaluate the efficacy of local GHG mitigation strategies as the city works toward its goal of becoming carbon neutral.

Our model–measurement framework includes several innovations which will be important to leverage for future inversions of tower and satellite data. One key development is constructing a $CO_2$ concentration curtain, tied to surface measurements but varying with altitude, which improved the agreement between the average modeled and observed enhancements by ∼40% compared with a simple difference method. This study also used a detailed representation of urban biological fluxes (which are typically zero in MODIS-based biological flux models), finding that the urban biosphere took up over half of the anthropogenic $CO_2$ emissions that reached the Boston sites on summer afternoons. Without representation of urban biological fluxes, accurate calculation of inverse emissions in cities was not possible during at least the 5 mo during the growing season. As NASA's Orbital Carbon Observatory-2 (OCO-2) satellite and the future OCO-3 and Geostationary Carbon Observatory (GeoCarb) satellites provide increasingly robust GHG datasets, we have shown that a detailed assessment of biological fluxes, boundary tracer concentrations, and time delays for air to transit the region, must be included in inverse analyses to achieve successful emissions monitoring. These satellites will also be an important resource for the improvement of boundary tracer assessments in the future.

Our results also demonstrate that high-quality, spatially and temporally explicit prior inventories of anthropogenic emissions are essential to obtaining accurate emissions assessments. For our Boston sites, 5-km resolution of the prior inventory leads to a 15% underestimate of the $CO_2$ enhancement compared with 1-km resolution (30% in the winter). High-resolution inventories are important for any measurement site within a city or near strong emissions, to allow Lagrangian particles to sample the spatially variable emissions field; such sites are currently operating in several established monitoring networks (8–10). Hence, to obtain accurate emissions assessments from the growing number of urban measurement networks, it will be essential for local governments to also obtain comprehensive bottom-up emissions inventories. Cities are leading GHG reduction efforts, but most are not yet investing in such detailed inventories or emissions reduction validation. Our work has demonstrated that atmospheric observations coupled with high-quality, spatially resolved inventories provide the foundation for cities to rigorously assess their GHG mitigation strategies.

The Paris climate accord is dependent upon accurate accounting of emissions from each country; without good data to assess how well countries or cities are meeting their targets, the utility of the agreement breaks down. This study presented several advances to inverse modeling techniques and demonstrated that the resulting framework enables us to constrain emissions in Boston within ±18%. Improved transport models and remote sensing data should allow us to narrow this uncertainty. Similar frameworks could be applied around the world to verify emissions reductions goals and help cities and countries to meet their international commitments.

**ACKNOWLEDGMENTS.** We thank Elaine Gottlieb, John Budney, Bruce Daube, Nathan Phillips, and Bill Munger for help with the measurements. We thank Earth Networks, Inc. for providing Canaan, NH, $CO_2$ measurements. Funding for this study was provided by BU College of Arts and Sciences, the National Aeronautics and Space Administration through the Carbon Monitoring System Awards NNX16AP23G and NNH13CK02C and OCO-2 Grant NNX15AG91G, the National Oceanic and Atmospheric Administration Urban Award NA17OAR4310086, the Environmental Defense Fund Award 0161-7386621, the National Science Foundation Major Research Instrumentation Award AGS-1337512 and Model Development Award ATM-0830916, the Harvard University Dean's Innovation Fund, the Climate Change Sustainability Fund 373679, and Harvard Global Institute 373516.

1. Intergovernmental Panel on Climate Change (2014) Climate Change 2014: Synthesis Report *Contribution of Working Groups I, II and III to the Fifth Assessment Report of the Intergovernmental Panel on Climate Change*, eds Pachauri R, Meyer L (Intergov Panel Clim Change, Geneva).
2. Energy Information Administration (2013) *International Energy Outlook 2013* (US Dep Energy, Washington, DC), DOE/EIA-0484.
3. United Nations Department of Economic and Social Affairs Population Division (2014) *World Urbanization Prospects: The 2014 Revision, Highlights* (United Nations, New York), ST/ESA/SER.A/352.
4. Tabuchi H, Fountain H (June 2, 2017) Bucking Trump, these cities, states and companies commit to Paris accord. *NY Times*, Section A, p 12.
5. Gurney KR, et al. (2009) High resolution fossil fuel combustion $CO_2$ emission fluxes for the United States. *Environ Sci Technol* 43:5535–5541.
6. Gurney KR, et al. (2012) Quantification of fossil fuel $CO_2$ emissions on the building/street scale for a large US city. *Environ Sci Technol* 46:12194–12202.
7. Asefi-Najafabady, et al. (2014) A multiyear, global gridded fossil fuel $CO_2$ emission data product: Evaluation and analysis of results. *J Geophys Res Atmos* 119:10213–10231.
8. Feng S, et al. (2016) LA megacity: A high-resolution land-atmosphere modelling system for urban $CO_2$ emissions. *Atmos Chem Phys* 16:9019–9045.
9. Lauvaux T, et al. (2016) High-resolution atmospheric inversion of urban $CO_2$ emissions during the dormant season of the Indianapolis Flux Experiment (INFLUX). *J Geophys Res Atmos* 121:5213–5236.
10. McKain K, et al. (2012) Assessment of ground-based atmospheric observations for verification of greenhouse gas emissions from an urban region. *Proc Natl Acad Sci USA* 109:8423–8428.
11. Staufer J, et al. (2016) The first 1-year-long estimate of the Paris region fossil fuel $CO_2$ emissions based on atmospheric inversion. *Atmos Chem Phys* 16:14703–14726.
12. Mueller K, et al. (2017) Siting background towers to characterize incoming air for urban greenhouse gas estimation: A case study in the Washington DC/Baltimore area. *J Geophys Res Atmos* 122:2910–2926.
13. McKain K, et al. (2015) Methane emissions from natural gas infrastructure and use in the urban region of Boston, Massachusetts. *Proc Natl Acad Sci USA* 112:1941–1946.
14. Verhulst K, et al. (2016) Carbon dioxide and methane measurements from the Los Angeles megacity carbon project: 1. Calibration, urban enhancements, and uncertainty estimates. *Atmos Chem Phys Discuss*, 1–16.
15. Bréon F, et al. (2015) An attempt at estimating Paris area $CO_2$ emissions from atmospheric concentration measurements. *Atmos Chem Phys* 15:1707–1724.
16. DeCola P, WMO Secretariat (2017) An Integrated Global Greenhouse Gas Information System (IG3IS) (World Meteorol Org, Geneva), Bull 66(1).
17. Intergovernmental Panel on Climate Change (March 7, 2018) World Scientists, Local Leaders Map Research Agenda for Cities and Climate Change for Coming Years (Intergov Panel Clim Change, Geneva). Available at https://citiesipcc.org/news/press-release-world-scientists-local-leaders-map-research-agenda-for-cities-and-climate-change-for-coming-years/. Accessed April 22, 2018.
18. Stein AF, et al. (2015) NOAA's HYSPLIT atmospheric transport and dispersion modeling system. *Bull Am Meteorol Soc* 96:2059–2077.
19. Lin JC, et al. (2003) A near-field tool for simulating the upstream influence of atmospheric observations: The Stochastic Time-Inverted Lagrangian Transport (STILT) model. *J Geophys Res* 108:4493–4510.
20. Nehrkorn T, et al. (2010) Coupled weather research and forecasting-stochastic time-inverted Lagrangian transport (WRF-STILT) model. *Meteorol Atmos Phys* 107:51–64.
21. Gately CK, Hutyra LR (2017) Large uncertainties in urban-scale carbon emissions. *J Geophys Res Atmos* 122:11242–11260.
22. Hardiman BS, et al. (2017) Accounting for urban biogenic fluxes in regional carbon budgets. *Sci Total Environ* 592:366–372.
23. Gately CK, Hutyra LR, Sue Wing I (2015) Cities, traffic, and $CO_2$: A multidecadal assessment of trends, drivers, and scaling relationships. *Proc Natl Acad Sci USA* 112:4999–5004.
24. Potosnak M, et al. (1999) Influence of biotic exchange and combustion sources on atmospheric $CO_2$ concentrations in New England from observations at a forest flux tower. *J Geophys Res* 104:9561–9569.
25. Peters W, et al. (2007) An atmospheric perspective on North American carbon dioxide exchange: CarbonTracker. *Proc Natl Acad Sci USA* 104:18925–18930.
26. Gurney KR, et al. (2017) Reconciling the differences between a bottom-up and inverse-estimated $FFCO_2$ emissions estimate in a large US urban area. *Elem Sci Anth* 5:44.
27. City of Boston (2017) Climate Action Plan (City of Boston, Boston, MA). Available at https://www.boston.gov/departments/environment/climate-action-plan. Accessed April 22, 2018.